Ann. Geophys., 32, 499–506, 2014
www.ann-geophys.net/32/499/2014/
doi:10.5194/angeo-32-499-2014

Annales Geophysicae
Open Access

First negative system of N_2^+ in aurora: simultaneous space-borne and ground-based measurements and modeling results

K. Axelsson[1,2], T. Sergienko[1], H. Nilsson[1], U. Brändström[1], K. Asamura[3], and T. Sakanoi[4]

[1]Swedish Institute of Space Physics, Kiruna, Sweden
[2]Division of Space Technology, Luleå University of Technology, Kiruna, Sweden
[3]Institute of Space and Astronautical Science, Japan Aerospace Exploration Agency, Sagamihara, Kanagawa, Japan
[4]Planetary Plasma and Atmospheric Research Center, Graduate School of Science,Tohoku University, Aramaki, Aoba, Sendai, Japan

Correspondence to: K. Axelsson (katarina@irf.se)

Received: 29 September 2013 – Revised: 26 March 2014 – Accepted: 1 April 2014 – Published: 20 May 2014

Abstract. The auroral emission of the first negative system of N_2^+ at 427.8 nm is analyzed using simultaneous measurements from the ground with ALIS (Auroral Large Imaging System) and from space with optical (MAC) and particle (ESA) instruments of the Reimei satellite. The study has two main objectives. The first is validation of the absolute calibration of the ALIS and the Reimei MAC cameras. The other task is to evaluate different cross sections of the electron excitation of N_2^+ that are used for the modeling of the auroral 1N system emissions. The simultaneous measurements of the 427.8 nm emission by ALIS and Reimei imagers show excellent agreement, indicating that the calibration of the two instruments is correct. Comparison of the 427.8 nm emission intensity calculated using the incident electron flux measured by the Reimei particle instruments with intensities measured by the optical imagers show that the best match is reached with the cross section from Shemansky and Liu (2005).

Keywords. Atmospheric composition and structure (airglow and aurora)

1 Introduction

The auroral 427.8 nm emission, produced by the transition from the N_2^+ $(B^2\Sigma_u^+)$ state to the first vibrational level of the ground state N_2^+ $(X^2\Sigma_g^+)$, is caused by simultaneous electron impact ionization and excitation of molecular nitrogen in the ionosphere, and is one of the best understood emissions. The intensity of the first negative emission band of N_2^+ has been shown to be directly proportional to the energy dissipated into the atmosphere (Dalgarno et al., 1965), and can, together with other emissions, be used to deduce the atmospheric composition and characteristic energy of the precipitating particles (Hecht et al., 2006).

For nightside auroras, the only excitation mechanism, for the N_2^+ 427.8 nm emission, is direct electron impact of N_2. Even though it is a simple emission, with few processes involved, there is still some indeterminacy in model results, mostly due to uncertainties in the excitation cross section. Reviews of the electron impact cross section for the N_2 molecule have been made by several authors, as a result of many experimental and theoretical studies (e.g., Itikawa, 2006). The sum of the cross section for the production of the $X^2\Sigma_g^+$, $A^2\Pi_u$ and $B^2\Sigma_u^+$ states is usually assumed to be the total cross section for nondissociative ionization of N_2 into N_2^+. The partial ionization–excitation cross section for the three states has been seriously questioned, especially the magnitude of the cross section for the $B^2\Sigma_u^+$ state. Doering and Yang (1997) used electron scattering measurements and found that the $B^2\Sigma_u^+$ state contributes 9–10 % to the total N_2^+ cross section. Another analysis by Van Zyl and Pendleton (1995) using emission cross section measurements shows that the contribution is 14.5 %. Shemansky and Liu (2005) established the cross sections for electron impact ionization–excitation of N_2 $(X\Sigma_g^+)$ molecules into N_2^+ $(X^2\Sigma_g^+)$, $(A^2\Pi_u)$ and $(B^2\Sigma_u^+)$ states using ionization oscillator strengths derived from photoionization measurements, claiming that this method is the most accurate approach. They compare their own estimated values with the

two sets of previously determined cross sections mentioned above, and find that the difference between the cross sections can reach 50 %.

The relationship between intensity and energy flux can also be obtained experimentally. In order to determine the intensity of an auroral emission based on measured electron flux, the conversion factor or the excitation efficiency is needed. A study by Steele and McEwen (1990) presents a collection of measured and calculated excitation efficiencies, and shows that experimental measurements of the excitation efficiency differ by about 50 %. The reason for these differences is mainly due to the lack of simultaneous particle measurements and optical observations, and due to uncertainties in calibration of the instruments.

With the Reimei satellite it is possible to make measurements of the optical emissions at the same time as measuring the precipitating particles. This peculiarity of the Reimei satellite was used for intercalibration of the optical and particle measurements using an ionospheric model by Whiter et al. (2012). In this paper the intensity of the 1 PG bands of N_2 measured by the Reimei camera was compared with the modeled intensity of the 1 PG bands calculated using the simultaneous measurements of the auroral electron spectra. The strong discrepancies between the observed and calculated results were demonstrated. The authors attributed this disagreement to the possible input of the other auroral emissions in the measured intensity as well as to the effect of the ground albedo, which is difficult to take into account in the calculations.

The objective of this study is to use simultaneous measurements of the intensity of the 427.8 nm 1 NG emission from ALIS (Auroral Large Imaging System) and the intensity and electron flux from the Reimei satellite to intercalibrate the optical and particle measurements, and to evaluate different sets of cross sections and spectroscopic parameters to find the best fit to the experimental data.

2 Instrumentation

Optical data from space and in situ particle data were obtained with the Japanese micro-satelite, Reimei. The satellite is in a sun-synchronous orbit at an altitude of about ∼ 630 km. It carries a payload consisting of Electron/Ion energy Spectrum Analysers (ESA/ISA) (Asamura et al., 2003) and a Muti-Spectral Auroral Imaging Camera (MAC) (Obuchi et al., 2008; Sakanoi et al., 2003), which enables it to make multi-spectral optical measurements of the aurora and the precipitating particles simultaneously.

The MAC instrument is a three-channel camera system, used to simultaneously measure at wavelengths of 4280 (N_2^+ 1 NG), 5580 (O) and 6700 (N_2 1 PG). For the data used in this study the time resolution is 120 ms and the exposure time 60 ms. A sensitivity calibration of the MAC imagers

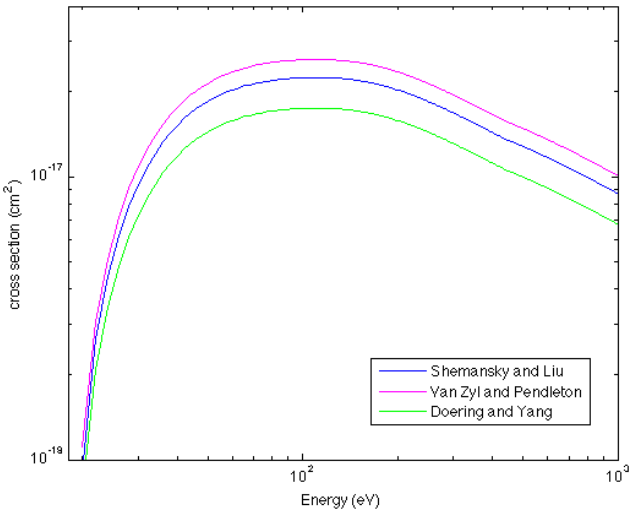

Figure 1. Partial ionization cross section for $N_2^+(B\,^2\Sigma_u^+)$.

was performed at the National Institute of Polar Research by using an integrating sphere (Obuchi et al., 2008).

The electron spectrometer, ESA, measures precipitating electrons in 32 energy bins covering a range from 12 eV to 12 keV, and records a complete electron energy spectrum every 40 ms. The ESA analyzer response for incoming direction and energy of the particles has been calibrated at the ground before launch by using ion beams (Asamura et al., 2003).

Optical data from the ground were obtained with ALIS (Brändström, 2003), which consists of several remote-controlled stations located in northern Scandinavia, separated by approximately 50 km. Each station is equipped with a high-resolution CCD detector with 1024 × 1024 pixels, and a filter wheel with six positions for narrow-band interference filters. The ALIS imager absolute calibration was carried out using the low-light radiative sources that are traceable to the long-term intercalibration effort (Brändström et al., 2012).

In this study we use data from the northernmost station in Skibotn (69.35° N, 20.36° E), Norway, where we have data at zenith coinciding with a pass of the Reimei satellite. The field-of-view is 90°, which with a binning of 4 × 4 pixels gives an image size of 256 × 256 pixels, and a spatial resolution of approximately 700 m at an altitude of 110 km. We use a 427.8 nm filter with 1 s exposure time. The time interval between the images using this filter is 15 s, which means one image was taken during the pass of the satellite, in which the footprint lies within the field of view of the ALIS imager.

3 Theory and modeling

The 427.8 nm emission belongs to the first negative band system of N_2^+. This system originates from the allowed electronic transition from the $B^2\Sigma_u^+$ state to the $X^2\Sigma_g^+$ state. In

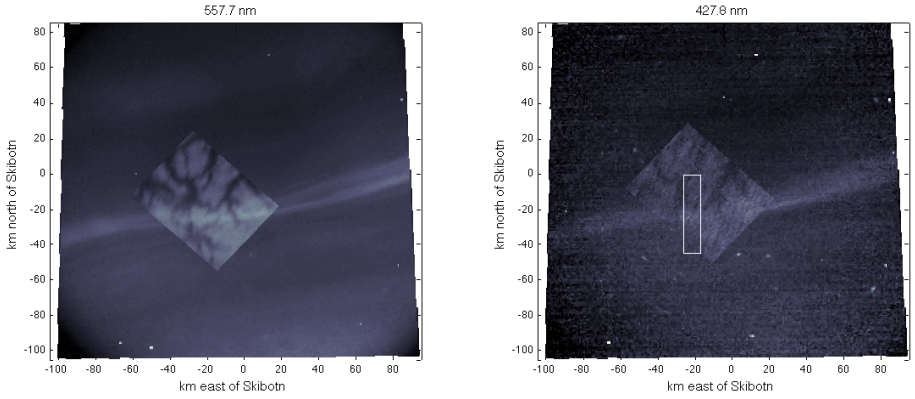

Figure 2. Images of the auroral arc from the ALIS camera in Skibotn taken on 8 November 2008 at 00:34:55 and 00:35:05 UT, respectively. On top is the average of 25 Reimei images taken between 00:35:02 and 00:35:06. Both are projected to an altitude of 110 km. The white box corresponds to the area where the mean value of the intensity was calculated.

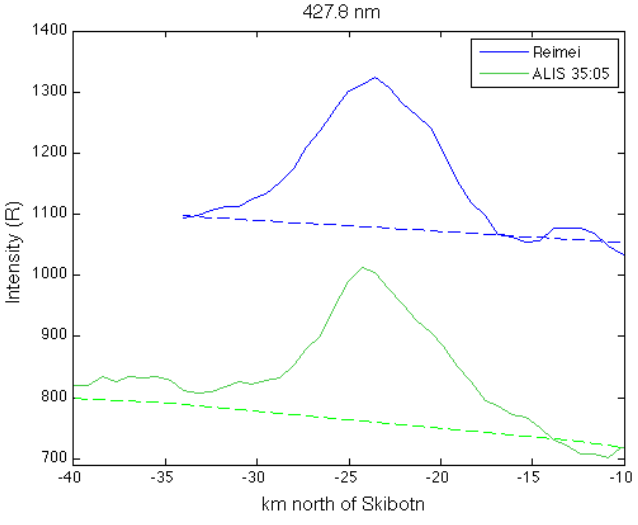

Figure 3. Intensity of the arc measured by ALIS and MAC before removing the background intensity. The dashed lines show the background intensity that is later removed from each intensity measurement.

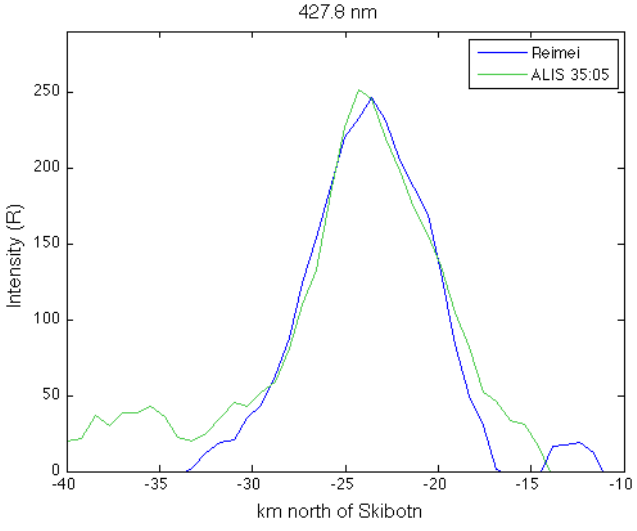

Figure 4. Intensity of the arc measured by ALIS and MAC after removing the background intensity.

aurora, the upper state is the result of electron impact ionization of nitrogen molecules with simultaneous excitation of N_2^+. The only loss process for the $B^2\Sigma_u^+$ state is by radiative transfer to the ground state. Therefore, under steady state conditions, the volume emission rate is defined as

$$V_{427.8}(z) = Q^{\nu=0}_{B^2\Sigma_u^+}(z) \cdot q^{0\to0}_{N_2(X)\to N_2^+(B)} \frac{A^{B\to X}_{0\to1}}{\sum_{\nu''} A^{B\to X}_{0\to\nu''}}, \quad (1)$$

where $V_{427.8}(z)$ is the volume emission rate of the 427.8 nm emission in $\mathrm{cm^{-3}\,s^{-1}}$, z is the altitude in cm, $q^{0\to0}_{N_2(X)\to N_2^+(B)}$ is the Franck–Condon factor for the transition from vibrational level $\nu' = 0$ of the ground state of N_2 to vibrational level $\nu'' = 0$ of the $N_2^+(B^2\Sigma_u^+)$ state, $A^{B\to X}_{0\to1}$ is the Einstein coefficient for the transition form vibrational level $\nu' = 0$ of the $B^2\Sigma_u^+$ state to vibrational level $\nu'' = 1$ of the $X^2\Sigma_g^+$ state of N_2^+ in $\mathrm{cm^{-1}}$, $\sum_{\nu''} A^{B\to X}_{0\to\nu''}$ is the sum of the Einstein coefficients of all transitions from vibrational level $\nu' = 0$ of the $B^2\Sigma_u^+$ state in $\mathrm{cm^{-1}}$, and $Q^{\nu=0}_{B^2\Sigma_u^+}(z)$ is the production rate of the $N_2^+(B^2\Sigma_u^+)$ state by the electron impact of N_2 in $\mathrm{cm^{-3}\,s^{-1}}$, and is calculated according to the following expression:

$$Q^{(\nu=0)}_{B^2\Sigma_u^+}(z) = [N_2(z)] \cdot \int_{E\mathrm{th}}^{\infty} \sigma_B(E) f(E,z) \mathrm{d}E, \quad (2)$$

where $[N_2(z)]$ is the N_2 number density in $\mathrm{cm^{-3}}$, $\sigma_B(E)$ is the electron-excitation cross section for the $N_2^+(B^2\Sigma_u^+)$ state

in cm^2, and $f(E,z)$ is the particle differential flux of the auroral electrons in $eV^{-1}\,cm^{-2}\,s^{-1}$.

The particle differential flux $f(E,z)$ can be obtained by solving the auroral electron transport problem. In order to solve this problem, we use the Monte Carlo model of the electron transport into the upper atmosphere of the Earth that was developed in Sergienko and Ivanov (1991) and updated according to the most recent laboratory measurements of the electron cross sections in Sergienko et al. (2012).

In spite of the simplicity of the modeling of the first negative system there are some problems associated with the uncertainty in the electron excitation cross section of the $N_2(B^2\Sigma_u^+)$ state. It is generally accepted that the partial ionization–excitation cross section of a certain electronic state of the molecular nitrogen ion is obtained from the total single ionization cross section by scaling according to the branching ratios (Shemansky and Liu, 2005). While the total ionization cross section is measured with high accuracy, the branching ratios for $X^2\Sigma_g^+$, $A^2\Pi_u$ and $B^2\Sigma_u^+$ are under debate. In Fig. 1 partial ionization cross sections for $B^2\Sigma_u^+$ are presented. In order to calculate these cross sections the total single ionization cross sections taken from Itikawa (2006) were used. The different cross sections correspond to the branching ratios presented by Van Zyl and Pendleton (1995) (green line), Doering and Yang (1997) (red line), and Shemansky and Liu (2005) (blue line).

One of the main goals of the present study is to evaluate these cross sections in order to find the best fit with the auroral measurements conducted simultaneously by space-borne and ground-based instruments. Some discrepancies exist in the values of spectroscopic parameters such as the Einstein coefficients and the Franck–Condon factors presented by the different authors. However, the differences in intensity using the different spectroscopic parameters are not significant compared to the difference obtained when changing the cross sections. In this study the values from Gilmore et al. (1992) are applied.

The volume emission rate of the auroral emissions related to the column intensity that is measured in the experiment by the following formula:

$$I_{427.8} = 10^{-6} \int V_{427.8}(z)\mathrm{d}z, \quad (3)$$

where $I_{427.8}$ is the column emission intensity in Rayleighs (R).

4 Experimental data and analysis

Since 2005 there have been around 60 conjugate measurements between ALIS and REIMEI. The majority of the conjugate observations had to be discarded due to a lack of geomagnetic activity, cloudy skies or various instrument malfunctions. Unfortunately only a few of them have been found to be useful for scientific analysis. Furthermore, there are no

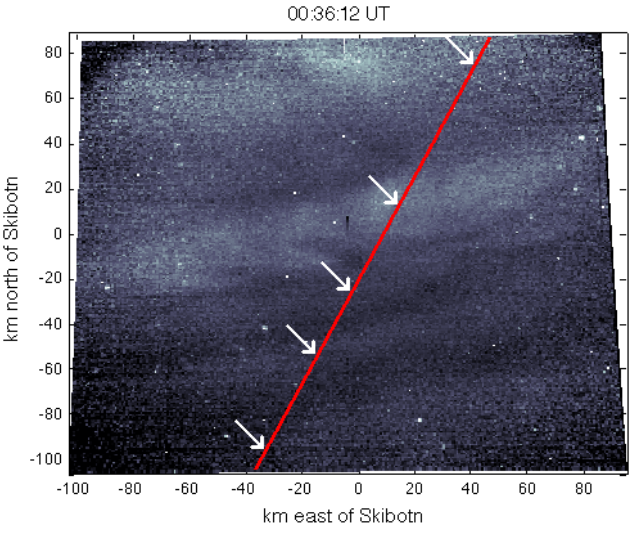

Figure 5. ALIS image (427.8 nm) from 5 December 2007 taken from the Skibotn station, projected to an altitude of 110 km. The red line marks the Reimei footprint and the white arrows point to the arcs.

observations where ALIS measures simultaneously with both optical and particle instruments on board Reimei. What does exist are simultaneous measurements of (1) ALIS and the optical imager on Reimei, (2) ALIS and particle measurements from Reimei, and (3) optical and particle data from Reimei. These three different combinations are used to compare the calibration of the instruments and investigate which of the cross sections gives the intensity that best matches the experimental data.

4.1 Comparison of optical data from ALIS and Reimei

A comparison of the intensity measured by the MAC instrument onboard Reimei and the ALIS camera in Skibotn was performed using data from 8 November 2008 at about 00:35:05 UT, when the fields of view of the two imagers overlap. We observe an auroral arc that lies in zenith and is stretched from east to west.

The 427.8 nm intensity of this arc is compared using measurements from the two imagers. Figure 2 shows the ALIS image for 557.7 nm (left) and 427.8 nm (right) projected to an altitude of 110 km with the MAC image superimposed. Since the arc is quite weak in intensity, especially in the blue line, we average 25 consecutive MAC images onto their common area, creating one image. There is no significant change in the shape or position of the arc during the time of two consecutive ALIS images, i.e., 15 s. The 25 images from the MAC instrument were obtained in the interval between two ALIS images and corresponds to 3 s, hence averaging the MAC images will not affect the result.

We find that there is a slight shift between the images, probably due to some uncertainties in the MAC imager

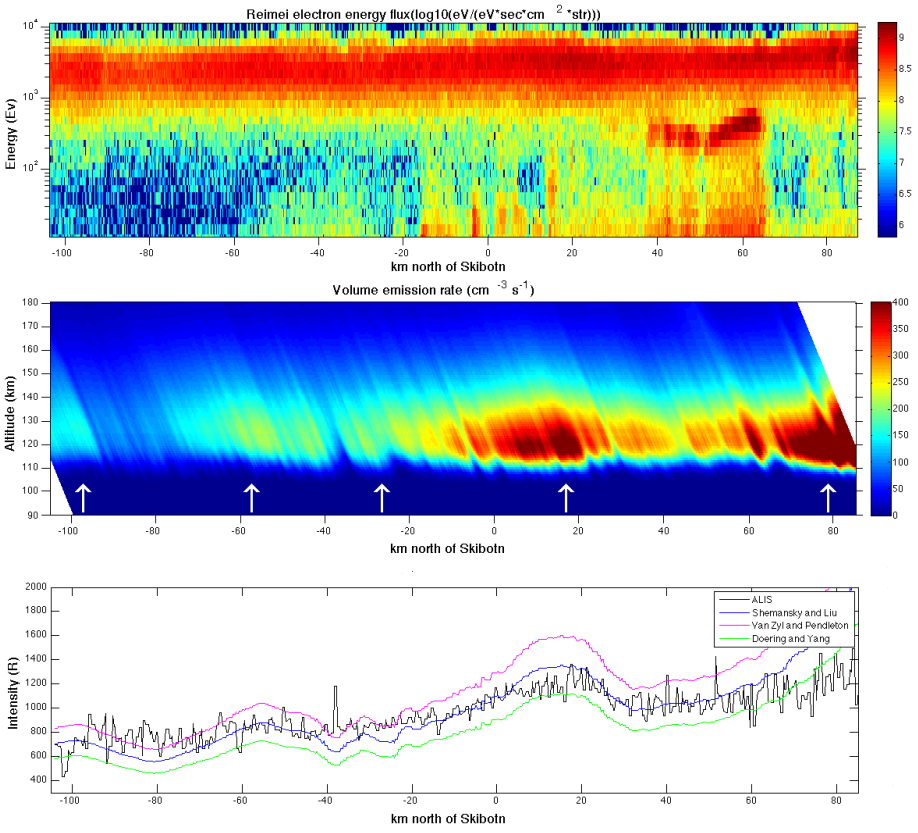

Figure 6. Upper panel: Electron energy spectrum along the track of the Reimei satellite. Middle panel: Volume emission rate as a function of altitude along the satellite track. The white arrows correspond to the arcs marked in Fig. 5. Lower panel: The black line shows the intensity of the 427.8 nm emission measured by ALIS. The three colored lines show the calculated intensity using cross sections from Van Zyl and Pendleton (1995), Shemansky and Liu (2005) and Doering and Yang (1997).

direction. We account for this inaccuracy by shifting the Reimei image 3.7 km to the north to obtain the best match for the position of the arc.

We include the image taken with the 557.7 nm filter, which is less noisy, to illustrate the conditions of the event better.

The intensity of the arc is calculated using 10 parallel slices of the image, taken along lines across the arc in a north–south direction starting from −27 to −17 km east of Skibotn with a spacing of 1 km. In order to increase the statistics we take the average of these lines and the result is found in Fig. 3.

The source of the background intensity in the ALIS image is background emissions that are always present in the night sky. For Reimei, these sources also include reflections of moonlight, starlight as well as the aurora itself from the ground. Since there is only one arc in the image, we calculate the background emissions by using the intensity obtained in the same way as described above, but for a line that is stretched from north to south across the whole image. We remove the area occupied by the arc, i.e., from around −32 to −13 km north of Skibotn, and fit a quadratic function to the remaining intensity. This resulting intensity is shown as the dashed line in the figure. Figure 4 shows the intensity of the arc after removal of the background intensity. We find that the measurements of the two imagers are in very good agreement. This supports the independent absolute calibration of the two camera systems.

4.2 Comparison of optical data from ALIS and particle data from Reimei

Optical data from ALIS is compared with particle data from Reimei, obtained on 5 December 2007, where the satellite data coincide with observations from the station in Skibotn (see Fig. 5).

The volume emission rate is calculated using Eqs. (1) and (2) for the three different sets of cross sections mentioned in Sect. 3. The middle panel of Fig. 6 shows the volume emission rate along the satellite track as a function of altitude. In this figure we see a peak of the volume emission rate at around 110–120 km in altitude.

The ALIS image in Fig. 5, taken with the 427.8 nm filter from the Skibotn station at 00:36:25, is projected to an altitude of 110 km, corresponding to the peak of the volume emission rate. The image show auroral structures that are

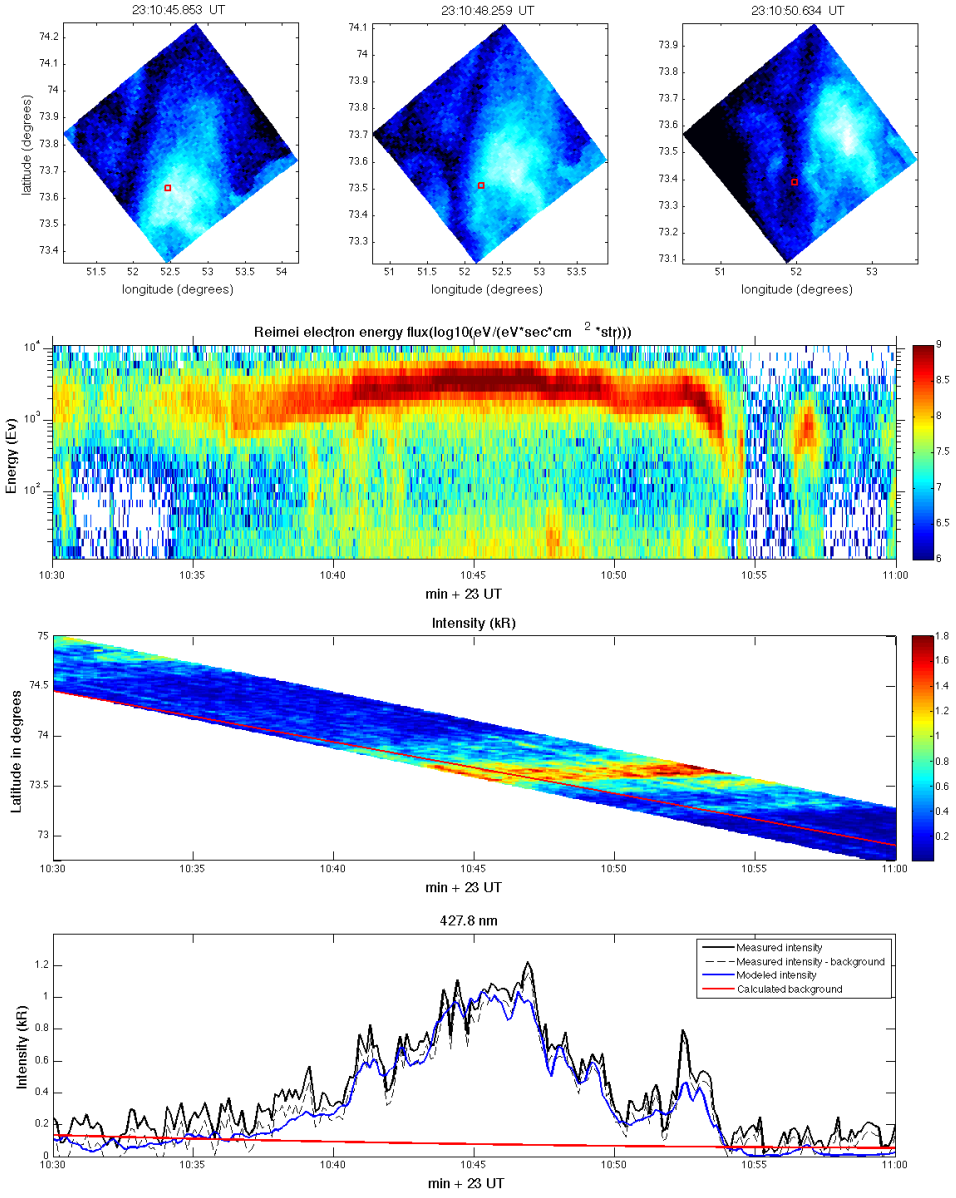

Figure 7. First panel: Images from MAC at three different times representing the event. The red square marks the satellite footprint. Second panel: Electron energy spectrum along the track of the satellite. Third panel: Keogram taken along the satellite track marked as the red line. Fourth panel: Measured and modeled intensity of the 427.8 nm emission together with the calculated background intensity.

elongated along the magnetic parallel. The image also shows the Reimei footprint (red line).

The energy spectrum along the satellite track is shown in the upper panel of Fig. 6 and shows a high flux in the 2–6 keV range along the whole track, which is in agreement with the diffuse auroral structures seen in Fig. 5. In the most northern part of the image there is also a population of accelerated electrons with lower energies of about 500–800 eV.

Finally the intensity is calculated using the volume emission rate and Eq. (3). The volume emission rate along the track is spread out along the magnetic parallel, creating a 3-D volume of the aurora. The 2-D image of this artificial aurora will be similar to Fig. 5, and is used to retrieve the intensity along the satellite track. The lower panel of Fig. 6 shows the intensity of the 427.8 nm emission along with the calculated intensity, based on the particle measurements, using the different cross sections.

The best agreement between the experimental data and calculated intensity is obtained by using cross sections from Shemansky and Liu (2005) together with spectroscopic parameters from Gilmore et al. (1992).

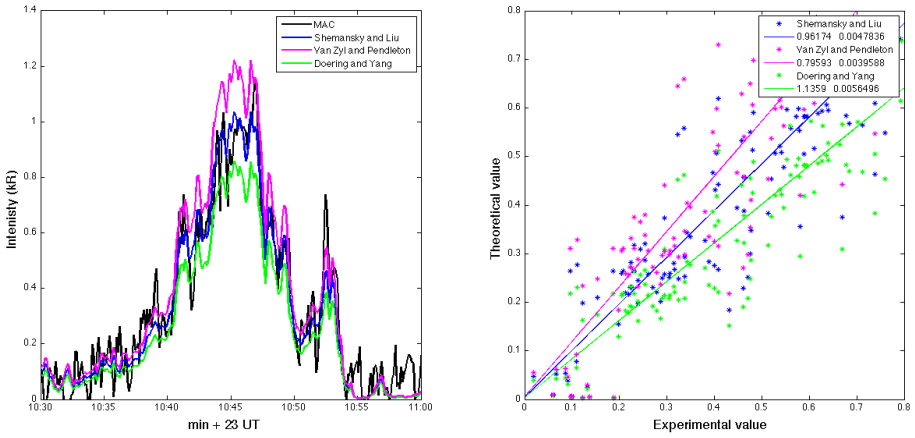

Figure 8. Left: Comparison between the measured intensity of 427.8 nm emissions and the modeled emission using cross sections from Shemansky and Liu (2005), Van Zyl and Pendleton (1995) and Doering and Yang (1997). Right: Linear regression plot between experimental and modeled intensities.

4.3 Comparison of optical and particle data from Reimei

Simultaneous optical and particle data from Reimei are of course much more common than Reimei–ALIS conjugate data. Our comparison of the ALIS and Reimei camera calibration shows that the Reimei camera is well-enough calibrated to be used for the quantitative comparison we are attempting here. We therefore investigate one sample event with simultaneous optical and particle measurements from Reimei. Data are taken from 9 December 2005 and are described in Fig. 7. Three images from the MAC imager representing the event are presented in the top panel and show the passing of an auroral structure. At around 23:10:46 the satellite footprint crosses the center of an auroral structure, which can be described as quite luminous and fairly stable. This can also be seen in the third panel of Fig. 7, which shows a keogram of the event, created by taking a slice along the satellite track for each image. Since the satellite is moving from north to south, each image will have a different latitude range and the resulting keogram will be tilted. The red line marks the footprint of the satellite.

The ESA spectogram of the precipitating auroral electrons is shown in the second panel of Fig. 7, and clearly indicates that the Reimei satellite passes several inverted V-like auroral structures formed by the electrons accelerated to an energy of 2–6 keV. The intensity of the 427.8 nm emission measured by MAC along the satellite footprint is shown in the third panel (black line). The background intensity is calculated by fitting a quadratic function to the lowest points of the measured intensity along the whole trace, and is included in the figure (red line). It also shows the modeled emission (blue line) using the ESA electron spectra with cross sections from Shemansky and Liu (2005).

We use the same set of cross sections as in Sect. 4.2 to calculate the intensity using the measured electron flux. The result is presented on the left side of Fig. 8 (colored lines), together with the measured intensity from MAC for the 427.8 nm emission (black line) after removing the background intensity. Similar to the ALIS-Reimei comparison the cross section from Shemansky and Liu (2005) gives a best fit of the experimental and calculated intensities. This fact is demonstrated more clearly on the right side of Fig. 8. The figure shows a linear regression plot of the dependence of the experimental values on the theoretical values for the three calculated intensities. The numbers in the legend are the coefficients obtained from the linear fitting between the experimental and theoretical values, where the first value represents the slope of the line, and the second term, the intercept that is close to zero for all three sets, indicate that the background calculations were correct. The blue line corresponding to cross sections from Shemansky and Liu (2005) has a regression coefficient of 0.96 and hence is the best mach to the measured intensity.

5 Conclusions

The intensities of the 427.8 nm emission measured from the ALIS and MAC imagers have been compared and show excellent agreement, indicating that the calibrations of the two instruments are correct.

We have compared the modeled intensity of the blue line using electron fluxes obtained from the ESA instrument using different cross sections and spectroscopic parameters with emission intensities measured by ALIS as well as MAC-Reimei. The best match is found using cross sections from Shemansky and Liu (2005).

As ALIS is traceable to the long-term intercalibration effort (Brändström et al., 2012), the agreement with the Reimei calibrated by independent facilities strengthens the quality of the optical absolute measurements of ALIS and Reimei.

Acknowledgements. K. Axelsson is supported by the Swedish National Graduate School of Space Technology, Luleå University of Technology. ALIS is supported by the Swedish Research Council.

Topical Editor K. Hosokawa thanks D. Lummerzheim and one anonymous referee for their help in evaluating this paper.

References

Asamura, K., Tsujita, D., Tanaka, H., Saito, Y., Mukai, T., and Hirahara, M.: Auroral particle instrument onboard the index satellite, Adv. Space Res., 32, 375–378, doi:10.1016/S0273-1177(03)90275-4, 2003.

Brändström, U.: The Auroral Large Imaging System: Design, Operation and Scientific Results, IRF scientific report, Swedish Institute of Space Physics (Institutet för rymdfysik), 2003.

Brändström, B. U. E., Enell, C.-F., Widell, O., Hansson, T., Whiter, D., Mäkinen, S., Mikhaylova, D., Axelsson, K., Sigernes, F., Gulbrandsen, N., Schlatter, N. M., Gjendem, A. G., Cai, L., Reistad, J. P., Daae, M., Demissie, T. D., Andalsvik, Y. L., Roberts, O., Poluyanov, S., and Chernouss, S.: Results from the intercalibration of optical low light calibration sources 2011, Geosci. Instrum. Method. Data Syst., 1, 43–51, doi:10.5194/gi-1-43-2012, 2012.

Dalgarno, A., Latimer, I., and McConkey, J.: Corpuscular bombardment and N_2^+ radiation, Planetary and Space Science, 13, 1008–1009, doi:10.1016/0032-0633(65)90160-1, 1965.

Doering, J. P. and Yang, J.: Direct experimental measurement of electron impact ionization-excitation branching ratios: 3. Branching ratios and cross sections for the N_2^+ $X^2\Sigma_g^+$, $A^2\Pi_u$, and $B^2\Sigma_u^+$ states at 100 eV, J. Geophys. Res.-Space, 102, 9683–9689, doi:10.1029/97JA00308, 1997.

Gilmore, F., Laher, R., and Espy, P.: Franck-Condon Factors, r-Centroids, Electronic Transition Moments, and Einstein Coefficients for Many Nitrogen and Oxygen Band Systems, J. Phys. Chem. Ref. Data, 21, 1005–1107, doi:10.1063/1.555910, 1992.

Hecht, J., Strickland, D., and Conde, M.: The application of ground-based optical techniques for inferring electron energy deposition and composition change during auroral precipitation events, J. Atmos. Sol.-Terr., 68, 1502–1519, 2006.

Itikawa, Y.: Cross Sections for Electron Collisions with Nitrogen Molecules, J. Phys. Chem. Ref. Data, 35, 31–53, doi:10.1063/1.1937426, 2006.

Obuchi, Y., Sakanoi, T., Yamazaki, A., Ino, T., Okano, S., Kasaba, Y., Hirahara, M., Kanai, Y., and Takeyama, N.: Initial observations of auroras by the multi-spectral auroral camera on board the Reimei satellite, Earth Planet. Space, 60, 827–835, 2008.

Sakanoi, T., Okano, S., Obuchi, Y., Kobayashi, T., Ejiri, M., Asamura, K., and Hirahara, M.: Development of the multi-spectral auroral camera onboard the index satellite, Adv. Space Res., 32, 379–384, doi:10.1016/S0273-1177(03)90276-6, 2003.

Sergienko, T. I. and Ivanov, V. E.: Transport of electrons in atmospheric gases. I – Integral characteristics, Geomagn. Aeronomy, 31, 635–642, 1991.

Sergienko, T., Gustavsson, B., Brändström, U., and Axelsson, K.: Modelling of optical emissions enhanced by the HF pumping of the ionospheric F-region, Ann. Geophys., 30, 885–895, doi:10.5194/angeo-30-885-2012, 2012.

Shemansky, D. E. and Liu, X.: Evaluation of electron impact excitation of N_2 $X^1\Sigma_g^+(0)$ into the N_2^+ $X^2\Sigma_g^+(v)$, $A^2\Pi_u(v)$, and $B^2\Sigma_u^+(v)$ states, J. Geophys. Res.-Space, 110, A07307, doi:10.1029/2005JA011062, 2005.

Steele, D. P. and McEwen, D. J.: Electron auroral excitation efficiencies and intensity ratios, J. Geophys. Res.-Space, 95, 10321–10336, doi:10.1029/JA095iA07p10321, 1990.

Van Zyl, B. and Pendleton, W.: N_2^+ (X), N_2^+ (A), and N_2^+ (B) Production in $e^- + N_2$ collisions, J. Geophys. Res.-Space, 100, 23755–23762, doi:10.1029/95JA02699, 1995.

Whiter, D., Lanchester, B., Sakanoi, T., and Asamura, K.: Estimating high-energy electron fluxes by intercalibrating Reimei optical and particle measurements using an ionospheric model, J. Atmos. Sol.-Terr., 89, 8–17, 2012.